INVESTIGATION OF X-RAY HARMONICS OF THE POLARIZED INVERSE COMPTON SCATTERING EXPERIMENT AT UCLA

A. Doyuran, O. Williams, R.J. England, C. Joshi, J. Lim, J.B. Rosenzweig, S. Tochitsky, G. Travish
UCLA Department of Physics and Astronomy, 405 Hilgard Ave., Los Angeles, CA 90095.

Abstract

An Inverse Compton Scattering (ICS) experiment, which will investigate nonlinear properties of scattering utilizing a terawatt CO_2 laser system with various polarizations, is ongoing at the UCLA Neptune Laboratory. When the normalized amplitude of the incident laser's vector potential a_0 is larger than unity the scattering occurs in the nonlinear region; therefore, higher harmonics are also produced. ICS can be used, e.g., for a polarized positron source by striking a thin target (such as tungsten) with the polarized X-rays. As such, it is critical to demonstrate the production of polarized scattered photons and to investigate the ICS process as it enters the nonlinear regime. We present the description of the experimental set up and equipment utilized, including diagnostics for electron and photon beam detection. We present the current status of the experiment.

INTRODUCTION

Inverse Compton Scattering (ICS) is becoming an effective source for producing third generation light source quality X-rays using low energy electron beams. For these light sources, and in HEP applications such as γ-γ colliders and polarized positron sources [1], an understanding of the physics of nonlinear and polarization dependent ICS is required.

The UCLA Neptune laboratory is an appropriate test bed for these experiments. Such experiments can utilize the existing terawatt CO_2 laser ($\lambda_L = 10.6$ µm), which, when strongly focused, may yield a normalized vector potential, $a_0 = eA_0 / m_e c^2 \cong 1$ where A_0 is vector potential of the laser field. In this regime, non-linear effects enter strongly in the interaction. The Neptune RF photo-injector gun and linac can deliver high quality electron beams having 14 MeV energy, 300 pC per bunch of 10 ps FWHM. Table 1 shows the designed electron and laser beam parameters and Table 2 shows the calculated scattered photon beam parameters for head on and transverse scattering cases [2-3]. Since both laser and electron beam require hard focusing into the IP, we have developed and built permanent magnet quadrupoles (PMQs) with 6 mm clear aperture. Even with a short distance to focus, the laser divergence makes head on scattering unfeasible. Therefore we have designed the scattering in transverse (90º) geometry.

EXPERIMENTAL SET UP

Figure 1 shows the schematic of the experimental set up in the ICS interaction chamber. The electron beam is focused by the PMQ system to the interaction point, and then recollimated by an identical PMQ system. The electron beam focusing and recollimating systems consist of 5 equal strength and length PMQs each, set up as a modified FF-DD-F triplet.

The high power CO_2 laser is focused by an off-axis parabolic mirror with a 12.7 cm diameter and 17 cm focal length. Since the divergence of the scattered photons is quite large (~$1/\gamma$, where $\gamma \cong 28$) it is necessary to place the detector (soft X-ray camera and/or micro-channel plate) very close to the IP. This requires bending the electron beam immediately after the recollimating PMQ system, in a very short bending radius. To this end, we have designed and built a permanent magnet dipole (PMD) with a ~60 mm bending radius for this purpose.

Table 1: Electron and Laser Beam Parameters

Parameter	Value
Electron Beam Energy	14 MeV
Beam Emittance	5 µm
Electron Beam Spot size (RMS)	25 µm
Beam Charge	300 pC
Bunch Length (RMS)	4 ps
Laser Beam Size at IP (RMS)	25 µm
CO_2 Laser Wavelength	10.6 µm
CO_2 Laser Rayleigh Range	0.75 mm
CO_2 Laser Power	500 GW
CO_2 Laser Pulse Length	200 ps

Table 2: Calculated Scattered Photon Parameters

Parameter	Head-on	Transverse
Scattered photon wave-length (fundamental)	5.3 nm	10.7 nm
Scattered photon energy	235.3 eV	117.7 eV
Scattered photon pulse duration (FWHM)	10 ps	10 ps
Interaction time	5 ps	0.33 ps
# of periods that electrons see (N_0)	283	10
# of photons emitted per electron (N)	3.34	0.11
Total # of photons	$6.3.10^9$	2.10^8
Half Opening Angle	2.7 mrad	15 mrad
Bandwidth	0.35%	10 %

Permanent Magnet Quadrupole (PMQ)

The ICS experiment requires that we produce a 25 μm (RMS) electron beam size at the IP. The ultra-short focal length quadrupoles which allow this type of focus consist of four NdFeB magnet cubes with 1.21 T resonant field, hyperbolic iron tips and hexagonal iron yoke for flux

0-7803-8859-3/05/$20.00 ©2005 IEEE

return (Fig. 2). The hyperbolic iron tips are held in place by an aluminum keeper which determines the geometric axis. The magnets are pushed towards the geometric axis by a screw to assure that they are equidistant from the center. This quadrupole produces ~115 T/m gradient.

Radia 3D magnetostatic simulations [4-5] are in good agreement with the measured gradient using a Hall probe. The magnetic axes of the PMQs are measured using a pulse wire measurement [6] and because the machining is done by electric discharge machining (EDM) we found the magnetic axis to be directly on the geometric axis within the accuracy of wire radius (25 µm).

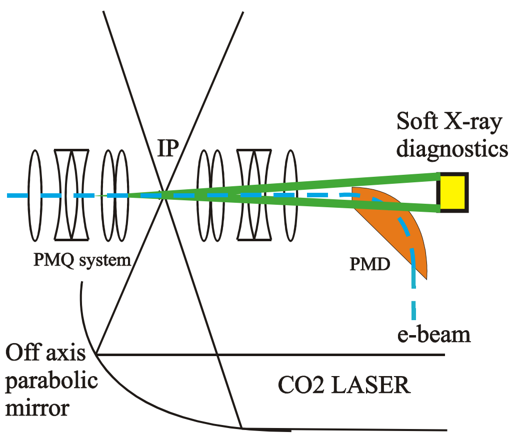

Figure 1: Focusing system for the electron and laser beams.

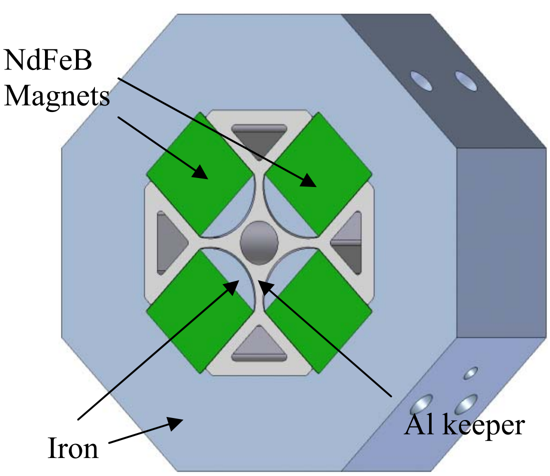

Figure 2: PMQ design using 4 cube magnets, hyperbolic pole tips and aluminum keepers.

Permanent magnet Dipole (PMD)

The typical opening angle of the scattered photon beam is ~$1/\gamma$ which requires having the soft-X-ray detector array very close to the IP. In order to bend the electron beam away from this detector in as short a distance as possible, immediately after the recollimating PMQs, a permanent magnet dipole (PMD) has been designed with bend angle of 90°.

The PMD, shown in rendered CAD format in Fig. 3, is designed such that the electron beam is bent 90^o vertically over a fairly wide range of energies. The nominal design energy bend radius is 60 mm. The magnet gap is 16 mm, and the magnetic material thickness is 30 mm with a magnetization of 1.32 T. This geometry provides the needed 0.78 T magnetic field inside the gap. The magnet and iron yoke is circularly cut to optimize the clearance for the scattered beam.

Radia simulations predict the measured fields very well. To accommodate beam off-axis, off-angle and off-energy operation we have placed the PMD on a remote controlled vertical mover. Thus the PMD can bend electron beams with energies ranging from 12 MeV to 14 MeV with various offsets in transverse positions and angles at the entrance of the PMD.

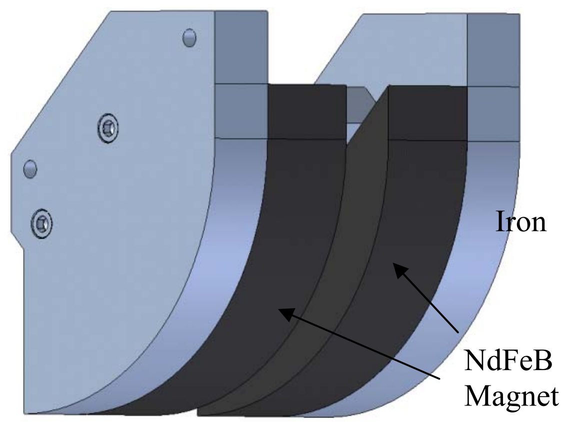

Figure 3: Compact dipole using permanent magnets.

IP Diagnostics

Dealing with 25 µm (RMS) beams at the IP requires careful imaging and alignment. The 90^o scattering geometry makes it difficult to image both electron and laser beams simultaneously. We designed and manufactured a pyramid shaped diagnostic (Fig. 4) with optically polished surfaces and sharp edges.

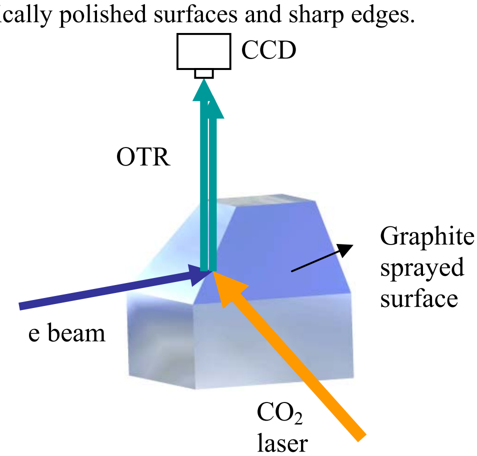

Figure 4: The IP imaging diagnostic "pyramid".

Transverse alignment is established by imaging the OTR from the electron beam and "sparking" from the

CO2 laser hitting a graphite layer applied to one pyramid surface. Simultaneous imaging two of the pyramid faces with a CCD allows for spatial alignment of the two beams. Temporal synchronization is established using a germanium crystal oriented at 45^o as a "gate". Incident beam electrons cause the germanium to become opaque to 10.6 μm radiation and block the perpendicularly incident CO_2 beam. Measurement of the corresponding transmitted intensity of the laser reveals the relative timing between the beams, allowing for tuning of the arrival time at the interaction point.

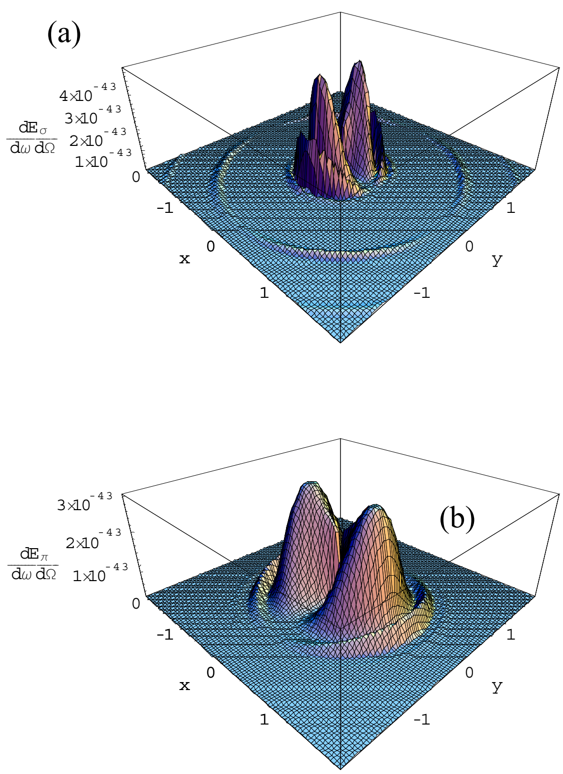

Figure 5: Intensity plot of σ (a) and π (b) polarizations at the first harmonic. The screen location is set at z=γ, and x and y are in mm units.

Calculation Tools

We have been working on a calculation tool which predicts the intensity distribution of the scattered photons for various laser polarizations and harmonics using a Mathematica routine. We use the algorithm described in Ref. 7. The reference describes only the head-on scattering case, which has since been generalized to the 90^o case [8]. These calculations produce full wavelength as well as angular spectra, and include features such as harmonic production and ponderomotive broadening.

Because the transverse case needed here is part of ongoing work, we only show (in Fig. 5) the intensity distribution of scattered photons from a Gaussian shape laser pulse for σ and π polarization of the first harmonic for 90^o case. The development of calculations for circular polarization with 90^o is now underway.

ELECTRON BEAM SIZE MEASUREMENT AT IP

We started running the experiment just recently and accomplished a measurement of the electron beam size at the IP using a YAG crystal. Preliminary measurement of the RMS beam size at the IP is about 40-50 μm for an 11 MeV electron beam which is not fully optimized. Our aim is to reduce the beam size to 25 μm at 14 MeV. An increase in energy will reduce the emittance due to the Schottky effect in the RF gun yielding a smaller spot size at the IP.

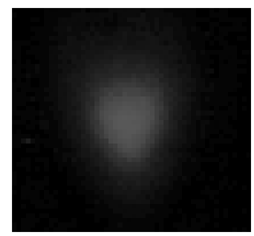

Figure 6: Electron beam image at the IP. RMS beam size is ~40-50 μm.

CONCLUSION

We have presented the details of the ongoing nonlinear polarized ICS experiment including design and calculation issues, and present status. The beam size measurements at the IP have proven the effectiveness of the PMQ focusing system, and represent a factor of 3 improvement over the original electromagnets.

REFERENCES

[1] T. Omori et. al., NIM A 500 (2003) 232-252
[2] S. Ride, E. Esarey, M Baine, Pyhs. Rev. E Vol 52, p5425 (1995)
[3] A. Doyuran, et.al., Study of X-ray Harmonics of the Polarized Inverse Compton Scattering Experiment at UCLA, AAC 2004 Proceedings.
[4] PAC97 Conference, Vancouver, May 1997: P. Elleaume, O. Chubar and J. Chavanne, "Computing 3D Magnetic Fields from Insertion Devices" (9P27)
[5] SRI97 Conference, SPring8, Japan, August 1997: O. Chubar, P. Elleaume and J. Chavanne, "A 3D Magnetostatics Computer Code for Insertion Devices"
[6] R. Warren, Nucl. Instrum. Methods Phys. Res. A272, 257 (1988)
[7] G. A. Krafft, Spectral Distributions of Thomson-Scattered Photons from High-Intensity Pulsed Lasers, PRL Vol 92 p 204802.
[8] G. A. Krafft, Pulsed Laser Nonlinear Thomson Scattering For General Scattering Geometries, to be submitted to PRST-AB

0-7803-8859-3/05/$20.00 ©2005 IEEE